Journal of Engineering Mathematics, Vol. 5, No. 4, October 1971
Wolters-Noordhoff Publishing–Groningen
Printed in the Netherlands

Wave Propagation from a Spherical Cavity Imbedded in an Elasto-Plastic Medium

J. ABOUDI

Department of Engineering Sciences, Tel Aviv University, Ramat Aviv, Israel.

(Received December 17, 1970)

SUMMARY

The problem of an impulsively applied pressure acting on the surface of a spherical cavity imbedded in an elasto-plastic medium governed by a bilinear stress-strain law is considered. The problem is solved by using a certain iterative finite difference scheme which prevents almost all the numerical oscillations which usually occur in the region behind the discontinuity at the elastic-plastic boundary, when a standard finite difference scheme is applied.

1. Introduction

The problem of spherical wave propagation produced by the application of a pressure to the surface of a cavity in elasto-plastic material has been investigated by several authors. Hopkins [1] gave a general review of the subject covering works published up to 1960. Friedman, Bleich and Parnes [2] determined the response of an elastic-perfectly incompressible plastic medium to an exponentially decaying pressure applied at the spherical cavity. This particular loading allowed a combined analytical and numerical approach employing a special finite difference scheme. Garg in [3] and [4] treated a similar medium using finite difference solution and series approximation for the starting of the solution. Davids, Mehta and Jhonson [5] used a direct numerical method for an elastic-incompressible plastic medium.

Mok [6] obtained the solution for perfectly plastic material using a finite difference solution with a scheme proposed by Lax [7] which adds to the original equation a linear viscosity term. As a result the discontinuity between the elastic and the plastic zones is smeared. This is also indicated by Chadwick and Morland [8]. Recently Yang [9] studied the propagation of waves in elastic-incompressible plastic material using the method of characteristics. In the present paper the problem of an impulsive non-decreasing pressure acting on the internal surface of a spherical cavity in an elasto-plastic medium is considered. The medium is assumed to behave according to a bilinear theory in which strain hardening and plastic compressibility can be taken into account. The constitutive equations for this theory are given by Aggarwal *et al.* [10]. According to these equations, the motion associated with the plastic region is coupled to that in the elastic region through the yield stresses, and this coupling reflects the intrinsic nonlinear character of the medium. The method of the solution in the plastic region is based upon a finite difference scheme in which an iterative procedure is used in order to remove oscillations which are typical for numerical calculations behind strong gradients such as shock waves. In our case these gradients occur between the elastic and plastic zones.

The present solution proves to be quite simple to apply, convenient, very effective and does not suffer from serious smearing of discontinuities. Results are given for the radial stress for different amounts of hardening, yielding and the applied pulse duration. The variation of position of the elastic-plastic boundary with time for several amounts of yielding and pulse duration is shown.

2. Statement of the Problem

Let us consider a spherical cavity of radius a in an infinite elasto-plastic medium. The material is considered to be isotropic, elasto-plastic with linear work hardening. The deformations are assumed to be small. The surface of the cavity is subjected to a time-dependent pressure $f(t)$

commencing at time $t=0$. We confine ourselves in this paper to the case of a continued loading, so that $f(t)\geqq 0$ for all $t\geqq 0$. We assume that the pressure $f(t)$ is such that the material adjacent to the cavity surface is at first deformed elastically and at a later time plastically.

The infinite region $r>a$ at some time $t>0$ is divided into the following three zones:

(1) A zone of loading $a<r<a+c_p t$ bounded by the cavity surface $r=a$ and terminating at the plastic wave front $r=a+c_p t$ which moves at the velocity of the plastic waves c_p given in the sequal.

(2) An elastic zone bounded by $r+c_p t<r<a+\alpha t$ which precedes the loading zone and terminates at the elastic wave front propagating at the elastic wave velocity α given in the sequal. At the boundary between the loading and elastic zones, discontinuities take place.

(3) The zone of the medium at rest: $r>a+\alpha t$.

Our purpose is to find the motion of the medium at $t>0$ as a result of the applied pressure on the surface of the cavity.

3. The Equations in the Elastic Zone

The constitutive equations at the elastic zone are given as usual by:

$$\sigma_{ij}=\lambda_1\varepsilon_{kk}\delta_{ij}+2\mu_1\varepsilon_{ij} \tag{1}$$

where σ_{ij}, ε_{ij} are the stress and strain tensors, δ_{ij} is the Kronecker delta, λ_1 and μ_1 are the Lamé's constants and ρ is the density.

According to the stress equations:

$$\rho\frac{\partial^2 u_i}{\partial t^2}=\sigma_{ij,j} \tag{2}$$

the elastodynamic equations of motion for the displacement vector $\boldsymbol{u}$ are:

$$(\lambda_1+2\mu_1)\,\text{grad div}\,\boldsymbol{u}-\mu_1\,\text{rot rot}\,\boldsymbol{u}=\rho\frac{\partial^2\boldsymbol{u}}{\partial t^2} \tag{3}$$

The longitudinal and shear wave velocities are given by

$$\begin{aligned}\alpha&=[(\lambda_1+2\mu_1)/\rho]^{\frac{1}{2}}=\left[\frac{3K_1(3K_1+E_1)}{\rho(9K_1-E_1)}\right]^{\frac{1}{2}}\\ \beta&=(\mu_1/\rho)^{\frac{1}{2}}=\left[\frac{3K_1E_1}{\rho(9K_1-E_1)}\right]^{\frac{1}{2}}\end{aligned} \tag{4}$$

where E_1 and K_1 are the elastic and bulk moduli respectively.

In the present case of spherical symmetry, (3) reduces to

$$\frac{1}{\alpha^2}\frac{\partial^2}{\partial t^2}u_r=\frac{\partial^2}{\partial r^2}u_r+\frac{2}{r}\frac{\partial}{\partial r}u_r-\frac{2}{r^2}u_r \tag{5}$$

where $\boldsymbol{u}=(u_r, 0, 0)$ in spherical coordinates (r, θ, ϕ) with the origin at the center of the cavity.

Before yielding takes place, equation (5) must be solved with the boundary condition:

$$\sigma_{rr}=-f(t)\ \text{ at }\ r=a\,. \tag{6}$$

4. The Equations in the Loading Zone

The plasticity equations of state, according to the bilinear theory [10] are given by:

$$\sigma_{ij}^{(2)}=\lambda_2\varepsilon_{kk}^{(2)}\delta_{ij}+2\mu_2\varepsilon_{ij}^{(2)} \tag{7}$$

and

$$\varepsilon_{ij}^{(2)}=\tfrac{1}{2}\left(\frac{\partial u_i^{(2)}}{\partial x_j}+\frac{\partial u_j^{(2)}}{\partial x_i}\right) \tag{8}$$

where the super index (2) denotes quantities added in the plastic region, and λ_2, μ_2 are the Lamé's constants for this region.

Then:

$$\sigma_{ij} = \sigma_{ij}^{(0)} + \sigma_{ij}^{(2)} \tag{9}$$

$$\varepsilon_{ij} = \varepsilon_{ij}^{(0)} + \varepsilon_{ij}^{(2)} \tag{10}$$

where $\sigma_{ij}^{(0)}$, $\varepsilon_{ij}^{(0)}$ denote the stress and strain tensors at the yield point which it is fixed according to the yield condition.

The elasto-plastic equations of motion according to the stress equation (2) and (7), (8) are given by:

$$\boldsymbol{F}^{(0)}(\lambda_2 + 2\mu_2)\,\text{grad div}\,\boldsymbol{u}^{(2)} - \mu_2\,\text{rot rot}\,\boldsymbol{u}^{(2)} + \boldsymbol{F}^{(0)} = \rho\frac{\partial^2 \boldsymbol{u}^{(2)}}{\partial t^2} \tag{11}$$

where:

$$F_i^{(0)} = \sigma_{ij,j}^{(0)} \tag{12}$$

The plastic wave velocities similarly to (4) are given by

$$\begin{aligned} c_p &= [(\lambda_2 + 2\mu_2)/\rho]^{\frac{1}{2}} = \left[\frac{3K_2(3K_2 + E_2)}{\rho(9K_2 - E_2)}\right]^{\frac{1}{2}} \\ c_s &= [\mu_2/\rho]^{\frac{1}{2}} = \left[\frac{3K_2 E_2}{\rho(9K_2 - E_2)}\right]^{\frac{1}{2}} \end{aligned} \tag{13}$$

E_2 and K_2 are the constant rate of work-hardening and the bulk modulus in the plastic region respectively. In Fig. 1 the bilinear stress-strain curve in simple tension and the pressure-dilatation curve are shown. For the special case of plastic incompressibility $K_2 = K_1$. In a perfectly plastic medium $E_2 = 0$.

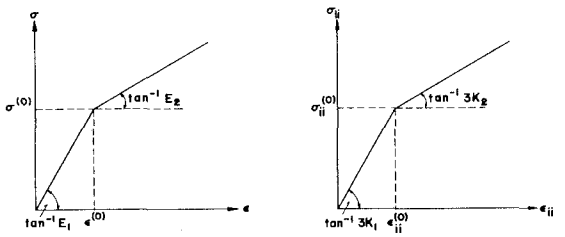

Figure 1. Bilinear stress-strain curve and pressure-dilatation curve.

Equations (11) show that the motion in the plastic region is coupled to that in the elastic region through the stresses at the yield point. This coupling reflects the intrinsic nonlinear character of the medium.

In the present case of spherical symmetry (11) reduces to

$$\frac{1}{c_p^2}\frac{\partial^2}{\partial t^2}u_r^{(2)} = \frac{\partial^2}{\partial r^2}u_r^{(2)} + \frac{2}{r}\frac{\partial}{\partial r}u_r^{(2)} - \frac{2}{r^2}u_r^{(2)} + F_r^{(0)}/\rho c_p^2 \tag{14}$$

Equation (14) must be solved with the boundary condition:

$$\sigma_{rr} = -f(t) \text{ at } r = a\,. \tag{15}$$

Then according to (9)

$$\sigma_{rr}^{(2)} = -[f(t) + \sigma_{rr}^{(0)}] \text{ at } r = a\,. \tag{16}$$

5. The Time-Dependent Pressure

We consider the case of an impulsive pressure $f(t)$ applied on the internal surface of the cavity. The function $f(t)$ is chosen as:

$$f(t) = A(1-e^{-\Delta \cdot t})H(t) \tag{17}$$

where $H(t)$ is the Heaviside step function, $1/\Delta$ is a time constant which determines the pulse duration and A is an amplitude factor having the dimension of stress, which corresponds to the maximum value that the pressure attains at $t\to\infty$. The function $f(t)$ given by (17) provides a gradually increasing pressure as a function of the time t. For $\Delta\to\infty, f(t)$ tends to $H(t)$. Various values of Δ provide the dependence of the elasto-plastic wave propagation upon the pulse duration.

6. The Yield Criterion

The yield criterion appropriate to linear work-hardening according to Hill [11] and Hopkins [1] is given by:

$$\left.\begin{aligned} &\sigma_{\theta\theta}-\sigma_{rr} = F(r, t, Y) \\ &F(r, t, Y) = Y+E_2\left(-\frac{\partial u_r}{\partial r}+\sigma_{\theta\theta}/3K_1-Y/E_1\right) \end{aligned}\right\} \tag{18}$$

where Y is the yield stress in uni-axial tension. σ_{rr}, $\sigma_{\theta\theta}$, $\partial u_r/\partial r$ are calculated by solving the elastic equation (5) with the boundary condition (6). For any time $t>0$ and radial distance $r\geqq a$, the stress difference $\sigma_{\theta\theta}-\sigma_{rr}$ is calculated by solving (5)–(6) to find whether the material has yielded. This is indicated by the yield function $F(r, t, Y)$ becoming equal to or greater than zero. Before the material has yielded, $F(r, t, Y)$ is negative. For a perfectly plastic material $E_2=0$ and the yield criterion (18) reduces to the simple form:

$$\sigma_{\theta\theta}-\sigma_{rr} = Y.$$

7. The Solution of the Elastic Equation

The solution of (5)–(6) is given by a convolution of the function $g(t)=(d/dt)f(t)$ with the solution $U_r(r, t)$ of (5) with the boundary condition:

$$\sigma_{rr} = -AH(t) \tag{19}$$

as given by Jeffreys [12] for $\alpha=\sqrt{3}\beta$. Thus:

$$u_r(r, t) = \int_0^t g(t-\tau)\,U_r(r, \tau)\,d\tau\,. \tag{20}$$

The result is:

$$\begin{aligned} u_r(r, t) &= A\frac{a^3\Delta e^{-\Delta\cdot t}}{4\mu_1 r^2}\left[(e^{\Delta t}-e^{\Delta(r-a)/\alpha})/\Delta+\sqrt{2}(r-a/2)\,C_2(r, t)/a\right. \\ &\quad \left.-C_1(r, t)\right]H(t-(r-a)/\alpha) \\ C_1(r, t) &= C\{e^{bt_1}[\sqrt{2}\sin\sqrt{2}t_1+b\cos\sqrt{2}t_1]-b\} \\ C_2(r, t) &= C\{e^{bt_1}[b\sin\sqrt{2}t_1-\sqrt{2}\cos\sqrt{2}t_1]+\sqrt{2}\} \\ C &= \frac{3a}{2\alpha}e^{(r-a)\Delta/\alpha}/(b^2+2),\ t_1 = 2(\alpha t-r+a)/3a,\ b=(3a\Delta-2\alpha)/2\alpha\,. \end{aligned} \tag{21}$$

8. Finite Difference Solution of the Equations in the Loading Zone

In the following we give a finite difference solution to (14) with the boundary condition (16). The term $F_r^{(0)}$ in (14) is calculated according to (12) and the elastic solution (21) at the yielding point by employing (18).

By replacing derivatives in (14) by central differences, the displacement at time $t+\Delta t$ is obtained in terms of its values at t and $t-\Delta t$:

$$u_r^{(2)}(r,t+\Delta t)=k^2[u_r^{(2)}(r+\Delta r,t)+u_r^{(2)}(r-\Delta r,t)]+k^2\frac{\Delta r}{r}[u_r^{(2)}(r+\Delta r,t)-u_r^{(2)}(r-\Delta r,t)]$$

$$-2\left[k^2+k^2\left(\frac{\Delta r}{r}\right)^2-1\right]u_r^{(2)}(r,t)-u_r^{(2)}(r,t-\Delta t)+(\Delta t)^2F_r^{(0)}/\rho \tag{22}$$

where: $k=c_p\Delta t/\Delta r$. (23)

The finite difference scheme (22) is applied at $r\geqq a$ and therefore a fictitious point is needed at $r=a-\Delta r$, the values at which are calculated using the boundary condition (16) as follows:

$$u_r^{(2)}(a-\Delta r,t)=[1+2(1-2c_s^2/c_p^2)\Delta r/a]u_r^{(2)}(a,t)+\Delta r[f(t)+\sigma_{rr}^{(0)}]/\rho c_p^2\,. \tag{24}$$

In order to find the appropriate stability condition for the three-time levels finite difference scheme (22), let us represent it in its equivalent two-time levels difference system as is shown in Richtmyer and Morton [13, p. 168–170]. This equivalent scheme can be written in the form:

$$\boldsymbol{w}(r,t+\Delta t)=[Q(\Delta t)+\Delta t\cdot Q_1(\Delta t)]\,\boldsymbol{w}(r,t) \tag{25}$$

where:

$$\boldsymbol{w}(r,t)=\begin{pmatrix}u_r^{(2)}(r,t)\\ x(r,t)\end{pmatrix},\quad u_r^{(2)}(r,t-\Delta t)\equiv x(r,t)$$

$Q(\Delta t)$ is the difference operator due to the second order derivative in r in (14) (the principle part), and $Q_1(\Delta t)$ represents the remaining terms.

According to Kreiss perturbation theorem [13,p.58], the difference system (25) is stable if the system:

$$\boldsymbol{w}(r,t+\Delta t)=Q(\Delta t)\,\boldsymbol{w}(r,t) \tag{26}$$

is stable, provided that $Q_1(\Delta t)$ is bounded.

Thus the stability condition for (22) can be founded by treating the principle part in (14) i.e.:

$$\frac{1}{c_p^2}\frac{\partial^2}{\partial t^2}u_r^{(2)}=\frac{\partial^2}{\partial r^2}u_r^{(2)}\,. \tag{27}$$

This is known [13,p.260–263] to be stable according to von Neumann, with the condition:

$$c_p\Delta t/\Delta r\leqq 1\,. \tag{28}$$

The finite difference scheme (22–24) is applied with $E_2=0.5\,E_1$, $K_2=0.6\,K_1$, $Y/A=0.2$, $a\Delta/\alpha=1$ and with a grid of $\Delta r=a/100$, $\Delta t=a/200\alpha$. The results for σ_{rr} as a function of the radial distance r are shown on the top of Fig. 2 at various times t. Nerve oscillations exist which begin near the shock front of the plastic wave. These oscillations are typical for numerical calculations behind strong gradients such as shock waves.

Mok [6] used a finite difference scheme proposed by Lax [7] which adds to the original equation a linear artificial viscosity term, and as a result the discontinuities between the loading and elastic zones are smeared and indistinct, which is an obvious disadvantage of the scheme.

Recently Abarbanel and Zwas [14] applied an iterative finite difference scheme to the problem of one dimensional time-dependent flow of a compressible gas in order to handle

discontinuities such as shock waves. They obtained monotonic profiles for almost all the cases they tested. Let us modify and apply their iterative method to our second order finite difference equation (22) in the following way:

Let $v(r, t) \equiv u_r^{(2)}(r, t)$ and

$$L[v(r,t)] = k^2\{v(r+\Delta r, t)+v(r-\Delta r, t)\} + k^2\frac{\Delta r}{r}\{v(r+\Delta r, t)-v(r-\Delta r, t)\}+$$

$$-2k^2\left\{1+\left(\frac{\Delta r}{r}\right)^2\right\} v(r, t)+(\Delta t)^2 F_r^{(0)}/\rho \tag{29}$$

Then (22) can be written in the form:

$$v(r, t+\Delta t) = 2v(r, t)-v(r, t-\Delta t)+L[v(r,t)] \tag{30}$$

Let us consider now instead of (30) the following iterative scheme in which the nth iteration v^n is obtained by:

$$v^n(r, t+\Delta t) = 2v(r, t)-v(r, t-\Delta t)$$
$$+\{w_3 L[v^{n-1}(r, t+\Delta t)]+w_2 L[v(r, t)]+w_1 L[v(r, t-\Delta t)]\}/(w_1+w_2+w_3) \tag{31}$$

where n is the order of the iteration, $n=1, 2, \ldots, N$; w_i are weight factors, and $v^0(r, t+\Delta t)$ is defined by:

$$v^0(r, t+\Delta t) = v(r, t+\Delta t) \tag{32}$$

where $v(r, t+\Delta t)$ is given by (30).

Actually (30–31) can be regarded as predictor-corrector, where (31) serves as the corrector and is applied several times each of which uses the results of the former steps. We choose weight factors w_i in (31) as; $w_1=-1$, $w_2=w_3=1$ which lead to the best results.

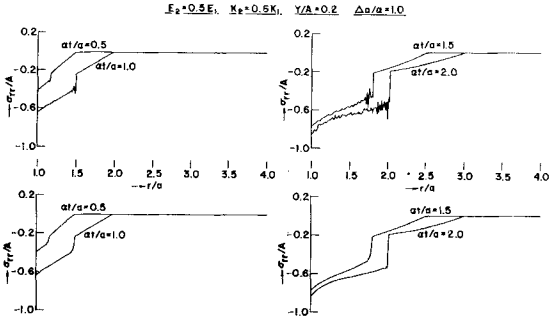

Figure 2. Radial stress variation with distance at various times, computed by the difference scheme (22) and (24) (top). Radial stress variation with distance, computed by the iterative scheme (31) and (24) (bottom).

The bottom of Fig. 2 shows the results with $N=1$, i.e., one iteration only. It is seen that the one iteration is highly effective in removing the oscillations, and does not have the disadvantage of serious smearing of discontinuities. Applying two iterations ($N=2$) gives results which are good as the results from the one iteration only, and up to the scale of the plot they are indistinguishable. In the sequel all the results are given with $N=1$.

Let us carry out the stability analysis of the iteration procedure with $N=1$. From (31) we get:

$$v^1(r, t+\Delta t) = [2+(\theta_2+2\theta_3)L+\theta_3 L^2]v(r, t)+[(\theta_1-\theta_3)L-1]v(r, t-\Delta t) \tag{33}$$

where: $\theta_i = w_i/(w_1+w_2+w_3)$, $(i=1,2,3)$.

We take again the principle part of (14). According to von Neumann let:

$$v(r, t) = v_0 e^{im\eta\,\Delta r}\xi^j \tag{34}$$

where $r=m\Delta r$, $t=j\Delta t$. Then (33) reduces to:

$$\xi^2 - 2A_1\xi + B_1 = 0 \tag{35}$$

where:

$$A_1 = 1 - 2(2\theta_3 + \theta_2)y + 8\theta_3 y^2 \tag{36}$$

$$B_1 = 1 - 4(\theta_3 - \theta_1)y \tag{37}$$

$$y = k^2 \sin^2 \frac{\eta \Delta r}{2}, \qquad k = c_p \Delta t / \Delta r \tag{38}$$

For stability, $|\xi| \leqq 1$ and therefore $|A_1| \leqq 1$ and $|B_1| \leqq 1$.
This implies that:

$$\theta_3 \geqq \theta_1, \quad \theta_3 \geqq 0, \quad (c_p \Delta t/\Delta r)^2 \leqq 0.5/(\theta_3 - \theta_1), \quad (c_p \Delta t/\Delta r)^2 \leqq (2\theta_3 + \theta_2)/4\theta_1 . \tag{39}$$

As stated above, the best results are obtained with $w_1 = -1$, $w_2 = w_3 = 1$, which clearly satisfy these conditions for stability if:

$$c_p \, \Delta t/\Delta r \leqq \tfrac{1}{2} . \tag{40}$$

9. Discussion

In Figs. 3–7 some results for the radial stress at different times are given for various values of the plastic parameters E_2, K_2. The effects of various values of yielding Y and time constants $1/\Delta$ are given, and the corresponding elastic-plastic boundaries are shown. In these figures the parameters are chosen such that: $w_1 = -1$, $w_2 = w_3 = 1$, $\Delta r = a/100$, $\Delta t = \Delta r/2\alpha = a/200\alpha$. This choice for Δt satisfies condition (40) because $c_p \leqq \alpha$.

Figs. 2–5 and Fig. (7) show the radial stress as a function of the distance r. They show the plastic region followed by the elastic region at a greater radial distance, with the discontinuity at the elastic-plastic boundary. The elastic region ends at the elastic wave front.

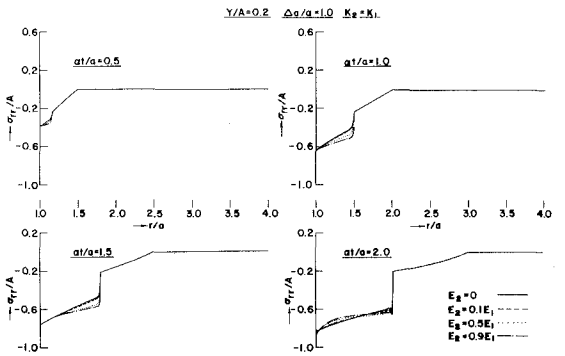

Figure 3. Radial stress variation with distance at various times, in the case of plastic incompressibility and different amounts of hardening.

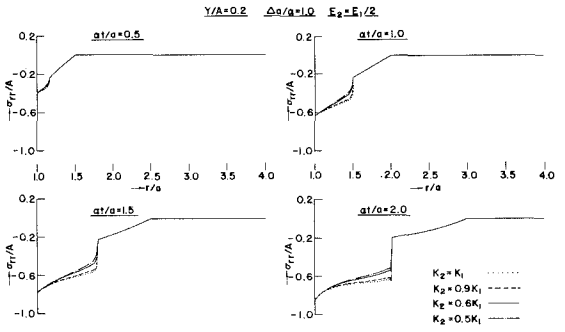

Figure 4 Radial stress variation with distance at various times, in the case of fixed hardening and different values of plastic bulk modulus.

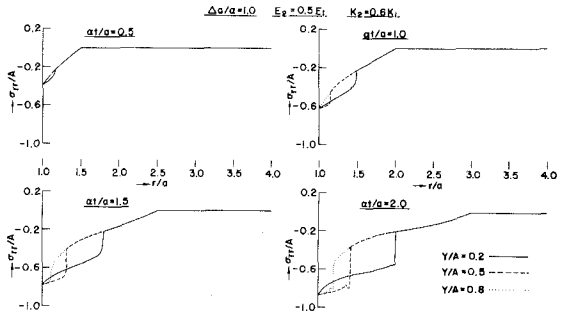

Figure 5. Radial stress variation with distance at various times, in the case of fixed time duration of the applied pulse and different amounts of yielding.

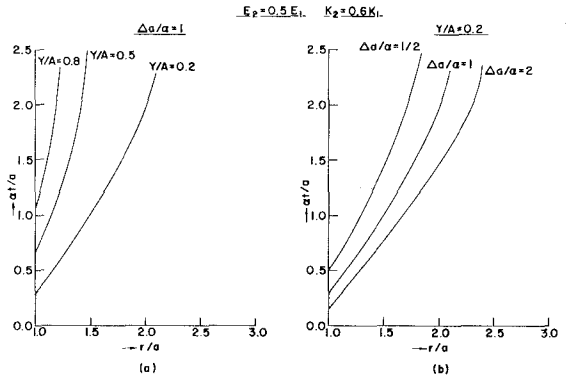

Figure 6. The propagation of the elasto-plastic boundary: (a) for different amounts of yielding; (b) for different values of pulse duration.

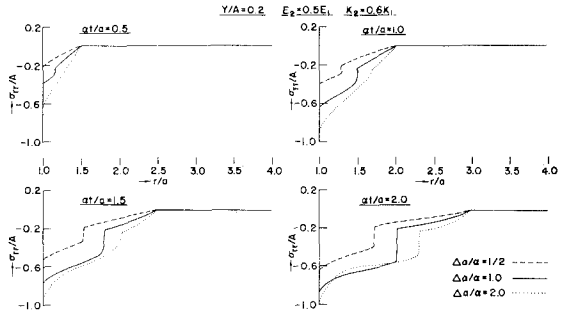

Fig. 7. Radial stress variation with distance at various times, in the case of fixed amount of yielding and different values of pulse duration.

Let us examine the effect of the change in E_2 and K_2 on the elasto-plastic wave propagation:
(a) In Fig. 3 the radial dependence of σ_{rr} is given at various times for the case of plastic incompressibility $K_2 = K_1$ and various amounts of hardening: $E_2/E_1 = 0, 0.1, 0.5, 0.9$. The solid line corresponds to a perfectly plastic medium. The results show that the effect of the hardening on σ_{rr} is not significant. See also Yang [9] who reaches the same conclusion.
(b) In Fig. 4 the radial stress is similarly examined for the case of fixed hardening $E_2 = E_1/2$ and different values of plastic bulk moduli: $K_2/K_1 = 1, 0.9, 0.6, 0.5$. Here again results show only slight changes of the radial stress σ_{rr} with K_2.

In Fig. 5 the radial stress is given for fixed time duration of the pulse and various amounts of yielding $Y/A = 0.2, 0.5, 0.8$. As could be expected the radial distance between the elastic front and the elasto-plastic boundary is shortened for lower amounts of yielding. In Fig. 6 the location of the elasto-plastic boundary at the various times, i.e. its propagation diagram, is given for

several values of yielding stresses Y and time constants $1/\Delta$. One can see clearly the effect of the applied pulse duration on the location of the boundary, showing that yielding in the material is dependent on the pulse duration as well as the applied pressure intensity. See also Hopkins [1]. This is also clearly seen in Fig. 7 where the radial stress is given for fixed amount of yielding $Y/A=0.2$ and different values of pulse duration $a\Delta/\alpha=0.5,1,2$.

Acknowledgement

The computations connected with this paper were performed at the Computations Center of Tel Aviv University.

REFERENCES

[1] H. G. Hopkins, Dynamic Expansion of Spherical Cavity in Metals, *Progress in Sold Mechanics*, 1, North-Holland Publishing Co., Amsterdam, 1960.
[2] M. B. Friedman, H. H. Bleich and R. Parnes, Spherical Elastic Plastic Shock Propagation, *J. Eng. Mech. Div. Am. Soc. Civ. Eng.*, 91 (1965) 189–203.
[3] S. K. Garg, Spherical Elastic-Plastic Waves, *Z. angew. Math. Phys.*, 19 (1968) 243–251.
[4] S. K. Garg, Numerical Solutions for Spherical Elastic-Plastic Wave Propagation *Z. angew. Math. Phys.*, 19 (1968) 778–787.
[5] N. Davids, P. K. Mehta and O. T. Johnson, "Spherical Elasto-Plastic in Materials", Materials, Behavior of Materials under Dynamic Loading, *Am. Soc. Mech. Engrs.*, (1966) 125–137.
[6] C. H. Mok, Dynamic Expansion of a Spherical Cavity in an Elastic, Perfectly Plastic Material, *J. Appl. Mech.*, 35 (1968) 372–378.
[7] L. Fox, *Numerical solution of Two-Point Boundary Problems*, Oxford (1957).
Appl. Math., 7 (1954) 159–193.
[8] P. C. Chadwick and L. W. Morland, The Starting Problem for Spherical Elastic-Plastic Waves of Small Amplitude, *J. Mech. Phys. Solids*, 17 (1969) 419–436.
[9] C. Y. Yang, Strain Hardening Effects on Unloading Spherical Waves in an Elastic Plastic Medium, *Int. J. Solids Structures*, 6 (1970) 757–772.
[10] H. R. Aggarwal, A. M. Soldate, J. F. Hook and J. Miklowitz, Bilinear Theories in Plasticity and an Application to Two-Dimensional Wave Propagation, *J. Appl. Mech.*, 31 (1964) 181–188.
[11] R. Hill, *The Mathematical Theory of Plasticity*, Clarendon Press, Oxford England (1950).
[12] H. Jeffreys, On the Cause of Oscillatory Movement in Seismograms, *Monthly Not. Roy. Astr. Soc. Geophys. Suppl.*, 2 (1931) 407–416.
[13] R. D. Richtmyer and K. W. Morton, *Difference Methods for Initial Value Problems*, Interscience, New York (1967).
[14] S. Abarbanel and G. Zwas, An Iterative Finite Difference Method for Hyperbolic Systems, *Math. Comp.*, 23 (1969) 549–565.